Microfluid Nanofluid (2007) 3: 47–53
DOI 10.1007/s10404-006-0104-9

RESEARCH PAPER

Rainer D. Jäggi · Roger Sandoz · Carlo S. Effenhauser

Microfluidic depletion of red blood cells from whole blood in high-aspect-ratio microchannels

Received: 4 April 2006 / Accepted: 18 May 2006 / Published online: 1 July 2006

Abstract A method for the depletion of red blood cells (RBCs) from whole blood at high volume flow rates is proposed and experimentally investigated. The approach exploits cell-screening effects at microchannel intersections with well-adjusted flow rates. It mimics blood flow phenomena previously observed and characterized in the microvascular system of living organisms. Because of the purely hydrodynamic nature of the depletion mechanism, the structural features on the device can be significantly larger than the cell dimensions in contrast to micromachined filter devices based on physical retention of cells/particles. Consequently, device fabrication is relatively straightforward and inexpensive. Cell depleted liquid can be withdrawn from the device in a continuous operation mode, thus avoiding the principal limitation of finite filter capacity associated with size exclusion based approaches. The use of high-aspect-ratio channels allowed for a combination of both cell screening action and high fluidic throughput in the ml/min regime. The experimental data relating flow velocities, channel dimension, cell depletion efficiency, and overall yield can be qualitatively interpreted using an adapted theoretical model originally developed by Fenton et al. Eventually, the method could serve as a simple, highly versatile pre-analytical sample preparation module for the manipulation of the particle density of suspensions in a miniaturized total analysis system.

Keywords Plasma separation · Red blood cells · Erythrocytes · Microfluidics · Plasma skimming

Rainer D. Jäggi · R. Sandoz · Carlo S. Effenhauser (✉)
Roche Diagnostics Microtechnology Center,
6343 Rotkreuz, Switzerland
E-mail: carlo.effenhauser@roche.com
Tel.: +41-41-7992487
Fax: +41-41-7992842

1 Introduction

The handling of suspensions and the manipulation of particle density represents a fundamental task in many biomedical applications, lately also being addressed by microfabrication means in miniaturized bioanalytical systems (Verpoorte 2003). Examples comprise the handling of dispersed beads added as a solid phase for heterogeneous biochemical assays, or the removal of blood cells from whole blood as an indispensable sample preparation step required for many in vitro diagnostic (IVD) tests in clinical diagnostics. The motivations for blood cell separation prior to IVD testing are diverse and range from inherently physiological to purely technical issues (for a comprehensive overview, see Guder et al. 1996). As an example of the latter, physical interferences due to light absorption/scattering from red blood cells (RBCs) or deposition onto electrode surfaces have to be avoided. Similarly, chemical interferences caused by inadvertent lysis of RBCs (hemoglobin) can deteriorate test performance (e.g., in PCR-based tests). RBC lysis is also known to lead to sample composition bias for analytes with a pronounced concentration difference between the intra- and extra-cellular compartments (e.g., K^+, acidic phosphatase, lactate dehydrogenase). Given this wide range of rationales, the required degree of cell depletion also scatters widely depending on the application under consideration.

In centralized clinical laboratories, blood cell separation is performed by centrifuges, a process known to add considerably to the labor, cost, and time requirements of an analytical result. In Point-of-Care (POC) settings (patient self-testing at home, physician office, hospital, etc.), with centrifuges generally not being available, plasma separation usually has to be integrated into the test device. Size-exclusion based retention of cells in an integrated microporous fleece or membrane material is the most commonly applied mechanism of operation, a formidable task in view of the small size and enormous deformability of RBCs.

High filter-performance and low fabrication cost are major advantages of this approach exploited in a number of commercially available POC tests. These advantages are challenged by the limited filter capacity and the risk of analyte adsorption due to the large inner surface area of the filter material. The latter issue may be appreciated by taking into account the analytical detection limit in the range of 10^{-12}–10^{-13} M for small proteins/peptides with current state-of-the-art devices.

Given the significant relevance of the task and the current interest in miniaturized and integrated bioanalytical systems, it is not surprising that quite a number of approaches were published aiming at micromachined particle filters. In particular, comb and weir-type structures with well-defined geometrical features have been designed and their performance experimentally tested (Wilding et al. 1994; Brody et al. 1996; He et al. 1999; Iida et al. 2002). However, in the case of RBCs, the extreme deformability requires a very small pore size in the order of 1 μm to retain these particles reliably, thus imposing a considerable challenge to the manufacturing process. In order to circumvent this issue, several groups have recently investigated RBC depletion in flow-through devices using microfluidic channels. Separation of cells from plasma was assisted by centrifugal forces in microchannel bends (Blattert et al. 2004) and spinning microfluidic discs (Burd and Schembri 1991; Brenner et al. 2004; Kang et al. 2004).

We have devised a concept for the depletion of RBCs from whole blood (Effenhauser et al. 2001, 2002) that exploits and mimics phenomena described in the context of blood flow in networks of branched blood capillaries in living organisms. Hydrodynamic effects rather than particle retention or application of additional external forces (e.g., centrifugal forces) cause cell depletion in a simple network of channel bifurcations. Fluid propulsion by conventional pressure-driven flow allows continuous withdrawing a particle-depleted solution. The general concept of hydrodynamic particle filtration has recently also been studied in detail using solid particles by Roberts and Olbricht (2006) and Yamada and Seki (2006). The enrichment of leukocytes in microchannels based on hydrodynamic filtration has been demonstrated by Yamada and Seki (2005). Shevkoplyas et al. have also reported leukocyte enrichment and separation due to collision induced margination in a pseudo 2D geometry (Shevkoplyas et al. 2005). Yang and Zahn have reported separation experiments at flow rate controlled channel bifurcations employing both solid particles and human melanoma cells (Yang and Zahn 2004). The same group has demonstrated separation of RBCs from blood in the 150 nl/min volume flow rate regime (Yang et al. 2005), a flow rate approximately a factor of 10 lower compared to an earlier study proving the underlying RBC separation concept (Effenhauser et al. 2002).

In the present study, we aim to extend the concept to flow rates several orders in magnitude higher (ml/min) by employing a high-aspect ratio channel bifurcation as a separation device. Essentially, one channel dimension will be kept small to retain the hydrodynamic basis of the cell screening process, while the other dimension can be chosen according to the throughput requirements of the application under consideration. As an important feature, the narrow channel dimension required can be significantly larger than the diameter of the particles to be depleted, thus significantly relieving both constraints in the fabrication process and the risk of clogging of the device. Using a straightforward method to manufacture high-aspect-ratio microchannels, we systematically characterized the yield and quality of the collected "plasma" as a function of volume flow ratio in the channel branches, sample hematocrit, channel dimensions, and feed volume flow rate. The data are discussed in the context of the model devised by Fenton et al. (1985), with modifications to reflect the particular geometry of our microchannels.

2 Hemodynamic effects in branched microchannels

Blood flowing through a bifurcation of artificial channels or branching microvascular vessels might be expected to give rise to identical concentrations of cells in each channel branch, provided the cells are equally distributed over the cross-section of the feed vessel. However, experimental data of the cell density does not follow this anticipation (Svanes and Zweifach 1968; Fung 1973; Yen and Fung 1978; Fenton et al. 1985; Yan et al. 1991; Enden and Popel 1994; Pries et al. 1996). Instead, the RBC flow rate (number of cells/s) in the channel branches depends non-linearly on the blood volume flow rate Q (m^3/s), even in the case of symmetric bifurcations and channels of identical cross-section (Svanes and Zweifach 1968; Fung 1973; Fenton et al. 1985). More specifically, the concentration of blood cells collected at the channel outlets is reduced in the branch with higher flow resistance (smaller volume flow rate). Below a critical flow rate Q_{crit}, even a stream of pure plasma can be obtained (Svanes and Zweifach 1968; Fung 1973; Fenton et al. 1985).

This type of separation of blood cells from blood plasma is related to purely hemodynamic phenomena that have been previously described in natural and artificial capillary bifurcations. Svanes and Zweifach (1968), by reducing the flow rate in arterioles, observed the depletion of RBCs in downstream vessels. Fung (1973) proposed the "stochastic flow in capillaries" model where small variations in the ratio of flow rates in branches emerging from a bifurcation determine whether a cell is deviated into one or the other branch. The concept of "red cell screening" proposed by Pries et al. (1996) relates to this observation: due to their finite size, cells and particles are subject to imbalanced fluid pressures at capillary bifurcations. The particle center trajectory may actually differ from the fluid streamlines in dilute samples, and particles are preferentially directed toward the stream with higher velocity.

The density distribution profile of blood cells across the channel cross-section is influenced by flow speed and channel dimension. The apparent hematocrit (blood cell volume fraction) and blood viscosity are functions of capillary diameter (Fåhraeus effect and Fåhraeus–Lindqvist effect, resp., Pries et al. 1996). In pressure driven flows, RBCs tend to migrate to the channel center (axial migration) due to pressure gradients imposed by the non-uniform flow velocity profile across the channel (Bayliss 1959; Goldsmith and Mason 1961). Accordingly, the fluid adjacent to the channel walls is depleted from cells, and a zone of reduced RBC concentration, termed "plasma seam", is found close to the channel walls. Moreover, separation of the cell-depleted plasma layer from the main laminar stream ("plasma skimming") (Yan et al. 1991; Enden and Popel 1994) can be achieved by branching off fluid near the wall into a side channel. The virtual boundary layer of streamlines that divides blood flow is called "separation surface". Any particle moving within the volume on either side of the separation surface will flow into the corresponding daughter channel.

The three-dimensional shape of the separation surface has been calculated for Poiseuille flows for junctions of cylindrical capillaries (Yan et al. 1991; Enden and Popel 1994). Modeling the separation surface for our high-aspect ratio rectangular bifurcation is comparatively simple. Sufficiently far away from the bifurcation and neglecting edge effects (small dimension walls), it extends parallel to the wide dimension of the feed channel at a certain height α above the channel wall. In a steady state, cells flowing above α in the feed channel are branched off into the collection channel (Fig. 1). The magnitude of α relative to the channel depth t is expected to strongly influence the efficiency of blood cell depletion, while it is independent of the channel width w for high-aspect ratio channels, $w \gg t$.

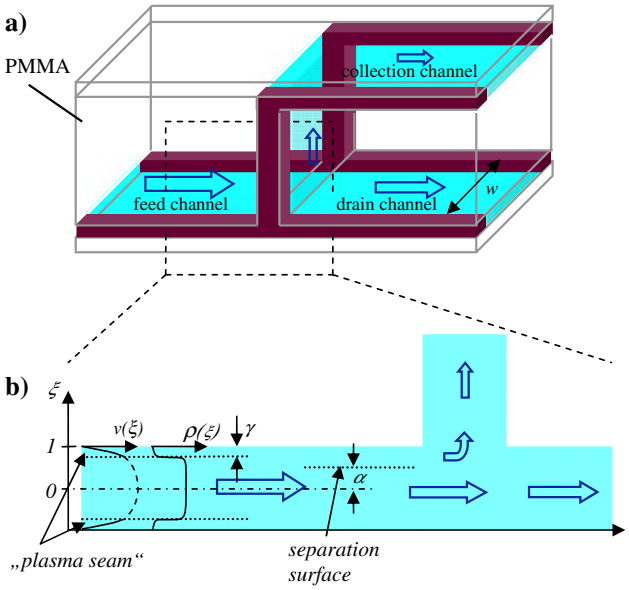

Fig. 1 **a** Schematic representation of the separation device with an inverted-T bifurcation. **b** Schematic representation of the flow velocity profile $v(\xi)$, the RBC distribution profile $\rho(\xi)$, the separation surface (defined by the height α), and volume flow distribution (*block arrows*) at the bifurcation. The relative thickness of the plasma seam is determined by γ. ξ is the normalized coordinate for the (half-) channel depth, with origin at the channel mid-plane

3 Device fabrication and experiments

A three-dimensional microchannel network in polymethylmetacrylate (PMMA) was manufactured by conventional precision machining. Wide and shallow channels of rectangular cross-section were milled into PMMA blocks and subsequently assembled using UV-curing adhesive to form an inverted T-bifurcation with one inlet (feed channel) and two outlets (collection and drain channel, Figs. 1, 2). The channel depth t was uniform throughout the network. Two types of devices were fabricated, differing in the depth t of the channels ($t = 0.02$ mm and $t = 0.05$ mm, respectively). The channel width ($w = 14$ mm) was much larger than the channel depth, with corresponding aspect ratios of $w/t = 700$ and 280, respectively.

Inlet and outlets were fitted with ports for the connection of standard tubing (inner tubing diameter 0.5 mm, Labomatic Instruments AG, Allschwil, Switzerland). A computer-controlled syringe pump (Kloehn V6, Kloehn Ltd. Europe, Switzerland) produced blood flow rates of 2 and 5 ml/min, respectively. The volume flow rate in the collection branch was tuned by changing the length of the connected tubing. The ratio of volume flow rates $Q^* = Q_{cc}/Q_{fc}$ of collection channel versus feed channel was adjusted in the range $0.01 < Q^* < 0.18$.

Blood samples were obtained from healthy donors and treated with EDTA to prevent coagulation. The hematocrit of the feed blood was adjusted using physiological saline solution (0.9% NaCl). Each experiment started with 10 ml of adjusted whole blood (hematocrit ~4.5, ~15, and ~45%).

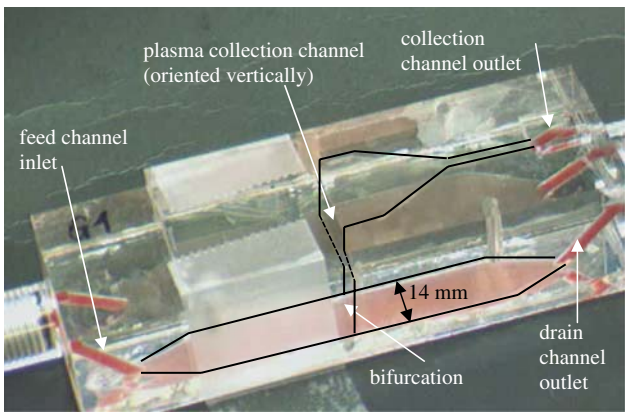

Fig. 2 Picture of the separation device with high-aspect ratio channels. Channel boundaries are outlined with *black lines* for clarity (optical refraction gives rise to multiple images of the feed and the drain channel)

The volume fractions used for the priming and emptying of the device (i.e. at the beginning and at the end of pumping of a 10 ml blood sample) were analyzed separately to elucidate the influence of device priming. Volume fractions taken once steady flow was established were analyzed as described below. Steady flow conditions were achieved within seconds after the pump start. The concentration of RBCs in the feed blood and in the blood collected at the channel outlets was determined using a blood cell counter (Sysmex F-820, Sysmex Corporation, Kobe, Japan).

Blood and plasma volumes collected at the channel outlets were determined by weighing. The ratio of weights was taken to correspond to the ratio of volume flows Q^*, neglecting differences in specific density arising from differences in hematocrit. Although Q^* is therefore systematically underestimated, the difference to the actual value is rather small. In the worst-case (45% feed hematocrit, pure plasma collected), the maximum error of the volume flow ratio Q^* is less than 5% on the basis of the measured specific density of blood plasma and blood cells (1,025 and 1,125 kg/m^3, respectively; see Kenner 1989). The error of Q^* is further reduced if the separation efficiency becomes smaller than 100%, and turns out to be well within the scatter of the experimental data.

4 Results and discussion

A striking feature of RBC depletion in capillary bifurcations is the non-linear relationship between RBC concentration c_{cc} and volume flow rate Q_{cc} in the collection channel. In Fig. 3, normalized concentration values $c^* = c_{cc}/c_{fc}$ are plotted as a function of the blood volume flow ratio $Q^* = Q_{cc}/Q_{fc}$ in the collection and the feed channel (symbols). Q^* describes the yield of RBC depleted blood relative to the initial blood volume. In the absence of any separation effects, the hematocrit collected at the channel outlets would equal the feed hematocrit, leading to $c^* = 1$ irrespective of Q^*.

In agreement with previous observations (Svanes and Zweifach 1968; Fung 1973; Fenton et al. 1985; Pries et al. 1996), blood with depleted RBC content was collected in the channel with higher flow resistance (collection channel). The concentration of RBCs in the collection channel approaches zero at decreasing flow rate ratio. The RBC depletion efficiency achieved in our high-aspect ratio device is in agreement with experiments using small capillaries (Fenton et al. 1985) and microchannels (Blattert et al. 2004), while sample throughput is significantly increased. Strikingly, with regard to the latter report of RBC depletion assisted by centrifugal action in bent microchannels (Blattert et al. 2004), a similar depletion efficiency is achieved in our devices even in the absence of centrifugal forces.

In order to gain a better understanding of the cell depletion process, we adapted a model by Fenton et al. (1985) to our high-aspect channel geometry. The theory

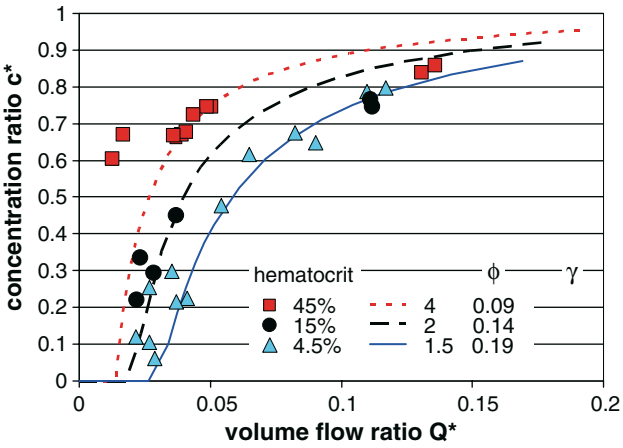

Fig. 3 Measured hematocrit ratio c^* as a function of volume flow ratio Q^* in the collection and the feed channel for different values of initial hematocrit (*symbols*). Fit of the "plasma skimming" model adapted from Fenton et al. (1985) (*lines*). φ corresponds to the viscosity ratio of plasma seam and RBC core, and γ is a measure of the plasma seam thickness relative to half of the channel depth. Channel depth $t = 0.05$ mm, flow rate 5 ml/min

describes the RBC depletion efficiency and volume yield as a function of the RBC number density ρ (number of cells/m^3) and the fluid velocity v (m/s) in the feed channel. For cylindrical channels, Fenton et al. modeled ρ by a cylindrical core of uniform RBC concentration, surrounded by a plasma seam with zero RBC content. Adapted to our channel geometry, the Fenton model predicts a step-like distribution function for ρ: a core layer of constant RBC density ρ_f is sandwiched between layers of cell-free plasma,

$$\rho(\xi) = \begin{matrix} \rho_f & \{|\xi| \le (1-\gamma)\}, \\ 0 & \{(1-\gamma) \le |\xi| \le 1\}. \end{matrix} \quad (1)$$

The thickness of the plasma seam γ is measured relative to half of the channel depth (Fig. 1b). Since the viscous properties of blood strongly depend on hematocrit, this RBC density profile implies regions of different viscosity in the channel. Modeling these regions as Newtonian fluids, the total velocity profile $v(\xi)$ is composed of region-specific parabolic flow profiles continuously joined at the boundaries between the RBC core and the plasma seam:

$$v(\xi) = \begin{matrix} (1-\gamma)^2 - \xi^2 + \phi\left(1-(1-\gamma)^2\right) & \{|\xi| \le (1-\gamma)\}, \\ \phi\left(1-\xi^2\right) & \{(1-\gamma) \le |\xi| \le 1\}. \end{matrix} \quad (2)$$

Here, $\varphi = \eta_{core}/\eta_{seam}$ is the viscosity ratio in the RBC core and the plasma seam. The volume flow rate Q_{fc} in the feed channel is determined by integration of $v(\xi)$ over the total channel cross-section area, while the flow in the collection channel Q_{cc} is integrated within $\alpha \le \xi \le 1$. The latter integration corresponds to the region delimited by the separation surface, i.e. the volume branched off in the "plasma skimming" process. Similarly, the RBC

flow rate in the feed and the collection channels are given by integration of the product $\rho(\xi)\cdot v(\xi)$ within the respective integration limits. The concentration ratio $c^* = c_{cc}/c_{fc}$ plotted in Fig. 3 is determined by the ratio of RBC flow rates divided by Q^*.

A qualitative fit of the "plasma skimming" model is obtained by adjusting the parameters φ and γ (Fig. 3). The viscosity of blood varies non-linearly as a function of hematocrit in the range of ~1.2 mPa/s for pure plasma to ~4.5 mPa/s for whole blood. Accordingly, for each hematocrit level, an initial approximation for φ was determined by the viscosity ratio of RBC core and plasma seam. For each hematocrit level, a set of curves was then calculated according to the Fenton model, each curve being associated with a fixed value of $\gamma = \gamma_i$ ($i = 1,...,25$, $\gamma_1 = 0.01$, $\gamma_2 = 0.02,...,\gamma_{25} = 0.25$). Parameter φ was then readjusted in steps of 0.1 around the initial value in order to observe the effect of variation of φ on the set of curves γ_i ($i = 1,...,25$). In this way, a qualitative fit was obtained by fixing φ and γ. Small variations of φ and γ resulted in an obviously inconsistent behavior of the fit with regard to the data. The three sets of optimized parameters γ and φ qualitatively reflect the anticipated increase of plasma seam thickness and decrease of the viscosity ratio with decreasing feed hematocrit (Fig. 3). The model predicts a stream of pure plasma ($c^* = 0$) below a critical flow ratio Q^*_{crit}.

A satisfactory qualitative fit is achieved despite the simplistic nature of the model (step-like RBC density profile, non-Newtonian flow behavior not taken into account), in particular for low feed hematocrit. At high feed hematocrit, fit and data agree less well, indicating the presence of effects not covered by the "plasma skimming" theory (cell collisions, cell screening, etc.). Experiments were conducted at rather high shear rates (up to 4,000/s), while Reynolds numbers are ≤ 5 (Table 1). Pries et al. (1996) predict that even at low Reynolds numbers, "particles do not always follow the fluid streamlines in which their center is located, leading to red cell screening at the bifurcation". For Reynolds numbers larger than 3, Fenton et al. (1985) observe reduced hematocrit in the collection branch, which cannot be reconciled with "plasma skimming" effects. In our experiments, however, η was only slightly affected by a factor 2.5 increase of the feed channel volume flow rate (Table 1).

Hemolysis of RBCs may be of particular concern due to high velocity gradients and shear stresses occuring in narrow channels and at high volume flows. The maximum wall shear stress is 57.1 Pa for 45% initial hematocrit (Table 1), well below reported thresholds for erythrocyte hemolysis (Sallem and Huang 1984). In addition, the total number of RBCs collected at both channel outlets was conserved, indicating negligible hemolysis in our devices.

The separation effect strongly depends on the concentration of RBCs in the feed channel. To help illustrate this effect, the separation efficiency is plotted as a function of feed hematocrit for a fixed volume flow ratio $Q^* \approx 0.037$ (Fig. 4). In agreement with the "plasma skimming" model, the separation efficiency improves with decreasing hematocrit. At smaller cell density, the flow velocity gradient across the channel is expected to increase, enhancing the migration of the cells toward the mid-plane of the channel (Bayliss 1959; Goldsmith and Mason 1961) and increasing the effective plasma seam thickness.

In agreement with earlier studies (Fenton et al. 1985), the RBC depletion efficiency improved with decreasing channel depth. At constant feed volume flow rate, the velocity gradient across a thinner channel increases, thus enhancing axial cell migration and increasing the contribution of cell-free plasma deviated into the collection channel. Experimental data for channel depth $t = 0.02$ and 0.05 mm are shown in Table 2. The separation efficiency substantially improved with decreasing channel depth, the improvement being more pronounced at high feed hematocrit. For diluted samples, the cell-depleted seam may already contribute substantially to the volume inside the separation surface, and an additional increase of the plasma seam thickness cannot be expected to further improve separation efficiency.

5 Conclusions

We have demonstrated a novel microfluidics-based method that allows for the controlled tuning of particle density of a suspension under high-throughput processing conditions. The device features simple channel intersections and can be easily integrated into planar device architecture as a versatile sample preparation module for various types of suspensions. Blood was depleted of RBCs with an efficiency that is in good agreement with previous experiments using small capillaries (Fenton et al. 1985) and bent microchannels

Table 1 Influence of feed volume flow rate on Reynolds number, wall shear stress, and cell depletion efficiency $\eta = 1 - c^*$

Initial hematocrit	Q^*	Reynolds number Re [wall shear stress (Pa)]		Separation efficiency η	
		$Q_{fc} = 2$ ml/min	$Q_{fc} = 5$ ml/min	$Q_{fc} = 2$ ml/min	$Q_{fc} = 5$ ml/min
4.5%	0.025	2 [8.6]	5 [21.4]	88%	92%
45%	0.04	0.6 [22.9]	1.4 [57.1]	31%	30%

Channel depth $t = 0.05$ mm

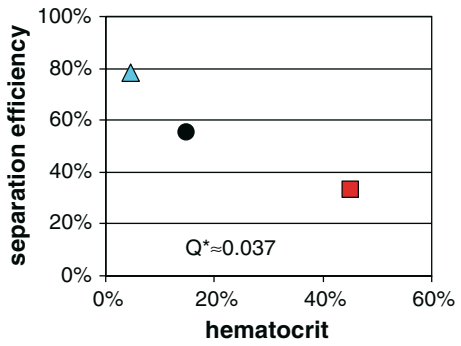

Fig. 4 Separation efficiency $\eta = 1 - c^*$ as a function of feed hematocrit for a fixed volume flow ratio ($Q^* = 0.037$). Channel depth $t = 0.05$ mm, flow rate 5 ml/min

(exploiting RBC depletion assisted by centrifugal forces, Blattert et al. 2004), while sample throughput was significantly increased by two orders of magnitude. Our wide, high-aspect ratio device may thus be regarded equivalent to many narrow channel bifurcations arranged in parallel. The separation process can be well described by an adaptation of a simple ''plasma skimming'' model despite its obvious simplifying assumptions (non-Newtonian flow behavior not taken into account, modeling of blood cell density distribution as a simple step function, etc.). RBCs may be completely depleted from whole blood using the proposed flow-through device, albeit at the cost of a strongly reduced volume yield.

The single bifurcation layout may be expanded to combinations of bifurcations with a linear (consecutive) or cascading series of collection channels. Sample fluid pumped through a linear series of bifurcations is continuously enriched in RBCs, since consecutive collection channels, preferably arranged on alternating sides of the feed channel, remove cell-depleted plasma. The flow resistance in the collection channels may be tuned such that plasma with the desired quality may be collected from consecutive bifurcations, increasing the total plasma yield. In a cascading combination of bifurcations, the cell-depleted sample collected at the first bifurcation is fed to a secondary bifurcation. Taking advantage of the increasing separation efficiency for samples with reduced hematocrit, plasma quality after the second and higher order bifurcations is improved. However, close inspection of the data shows that due to the non-linear dependence of the separation efficiency on volume flow ratio in the range $Q^* < 0.2$, a single, well-tuned bifurcation is generally more efficient in terms of plasma quality and yield.

Table 2 Influence of channel depth on cell depletion efficiency $\eta = 1 - c^*$

Initial hematocrit	Q^*	Separation efficiency η	
		$t = 0.02$ mm	$t = 0.05$ mm
15%	0.05	59%	42%
45%	0.07	37%	17%

Volume flow rate 2 ml/min

Acknowledgments We would like to thank Dr. G. Ocvirk, Roche Diagnostics Mannheim, Germany, for sharing his insights obtained with the first generation of microfabricated separation devices and helpful discussions, and Dr. Wolfgang Fiedler for his valuable contributions in the early phase of the project. Walter Meier and Hansruedi Müller, Roche Instrument Center, Rotkreuz, Switzerland, are acknowledged for designing and manufacturing of the microchannel devices.

References

Bayliss LE (1959) The axial drift of the red cells when blood flows in a narrow tube. J Physiol 149:593–613

Blattert C, Jurischka R, Schoth A, Kerth P, Menz W (2004) Separation of blood in microchannel bends. Proc SPIE 5345:17–25

Brenner T, Haeberle S, Zengerle R, Ducrée J (2004) Continuous centrifugal separation of whole blood on a disk. In: Proceedings of the 8th international conference on miniaturized systems in chemistry and life sciences (uTAS), Malmö, Sweden, 26–30 September 2004

Brody JP, Osborn TD, Forster FK, Yager P (1996) A planar microfabricated fluid filter. Sensor Actuator A 54:704–708

Burd TL, Schembri CT (1991) Apparatus and method for continuous centrifugal blood cell separation. Patent no. US 5186844

Effenhauser CS, Ocvirk G, Fiedler W (2001) Method and separation module for the separation of particles from a dispersion, in particular of blood corpuscles from blood. European Patent EP 1434637

Effenhauser CS, Ocvirk G, Fiedler W (2002) Major advances through miniaturization. In: Paeuser S (ed) Innovation, our key to success. Roche R&D Media Day, Penzberg, Germany, 24–25 April 2002. www.roche.com/pages/downloads/company/pdf/rddpenzberg02_02e.pdf

Enden G, Popel AS (1994) A numerical study of plasma skimming in small vascular bifurcations. J Biomech Eng 116:79–88

Fenton BM, Carr RT, Cokelet GR (1985) Nonuniform red cell distribution in 20 to 100 μm bifurcations. Microvasc Res 29:103–126

Fung YC (1973) Stochastic flow in capillary blood vessels. Microvasc Res 5:34–48

Goldsmith HL, Mason SG (1961) Axial migration of particles in Poiseuille flow. Nature 190:1095–1096

Guder WG, Narayanan S, Wisser H, Zawta B (1996) Samples: from the patient to the laboratory. GIT Verlag, Darmstadt

He B, Tan L, Regnier F (1999) Microfabricated filters for microfluidic analytical systems. Anal Chem 71:1464–1468

Iida K, Kawaura H, Iguchi N, Sano T, Baba M (2002) Planar ultra-filtration chip for rapid plasma separation by diffusion. In: Proceedings of the 6th international conference on miniaturized systems in chemistry and life sciences (uTAS), vol 2. Nara, Japan, 9–12 October 2002, pp627–629

Kang JY, Cho H, Kwak SM, Yoon DS, Kim TS (2004) Novel particle separation using spiral channel and centrifugal force for plasma preparation from whole blood. In: Proceedings of the 8th international conference on miniaturized systems in chemistry and life sciences (uTAS), Malmö, Sweden, 26–30 September 2004

Kenner T (1989) The measurement of blood density and its meaning. Basic Res Cardiol 84:111–124

Pries AR, Secomb TW, Gaehtgens P (1996) Biophysical aspects of blood flow in the microvasculature. Cardiovasc Res 32:654–667

Roberts BW, Olbricht WL (2006) The distribution of freely suspended particles at microfluidic bifurcations. AIChE J 52:199–206

Sallem AM, Huang NHC (1984) Human red blood cell hemolysis in a turbulent shear flow, contribution of Reynolds shear stress. Biorheology 21:783–797

Shevkoplyas SS, Yoshida T, Munn LL, Bitensky MW (2005) Biomimetic autoseparation of leukocytes from whole blood in a microfluidic device. Anal Chem 77:933–937

Svanes K, Zweifach BW (1968) Variations in small blood vessel hematocrit produced in hypothermic rats by micro-occlusion. Microvasc Res 1:210–220

Verpoorte E (2003) Beads and chips: new recipes for analysis. Lab Chip 3:60N–68N

Wilding P, Pfahler J, Bau HH, Zemel JN, Kricka LJ (1994) Manipulation and flow of biological fluids in straight channels micromachined in silicon. Clin Chem 40:43–47

Yamada M, Seki M (2005) Hydrodynamic filtration for on-chip particle concentration and classification utilizing microfluidics. Lab Chip 5:1233–1239

Yamada M, Seki M (2006) Microfluidic particle sorter employing flow splitting and recombining. Anal Chem 78:1357–1362

Yan ZY, Acrivos A, Weinbaum S (1991) A three-dimensional analysis of plasma skimming at microvascular bifurcations. Microvasc Res 42:17–38

Yang S, Zahn JD (2004) Particle separation in microfluidic channels using flow rate control. In: Proceedings of the ASME international mechanical engineering congress, Anaheim, CA, 13–19 November 2004, pp1–6

Yang S, Undar A, Zahn JD (2005) Biological fluid separation in microfluidic channels using flow rate control. In: Proceedings of the ASME international mechanical engineering congress, Orlando, 5–11 November 2005, pp1–7

Yen RT, Fung YC (1978) Effect of velocity distribution on red cell distribution in capillary blood vessels. Am J Physiol Heart Circ Physiol 4:H251–H257